# Supplementary Material

# A structural basis for Lowe syndrome caused by mutations in the Rab binding domain of OCRL1

Xiaomin Hou[1], Nina Hagemann[2], Stefan Schoebel[1], Wulf Blankenfeldt[3], Roger S. Goody[1], Kai S. Erdmann[2], Aymelt Itzen[1]

[1] Max-Planck-Institute of Molecular Physiology, Department of Physical Biochemistry, Dortmund 44227, Germany
[2] Ruhr-University Bochum, Department of Biochemistry II, 44780 Bochum, Germany
[3] University of Bayreuth, Department of Biochemistry, 95447 Bayreuth, Germany

For correspondence:
Aymelt Itzen, Ph.D.
Max-Planck-Institut für Molekulare Physiologie
Abt. Physikalische Biochemie
Otto-Hahn Str. 11, Dortmund 44227, Germany.
Tel.: +49 231 1332305
Fax: +49 231 1332398
E-mail: aymelt.itzen@mpi-dortmund.mpg.de

Kai S. Erdmann
PD Dr. Kai S. Erdmann
Ruhr-Universität Bochum
Biochemie II
Universitätsstraße 151, 44780 Bochum, Germany
Tel.: +49 234 32 26208
Fax: +49 234 32 14105

# Supplementary Figures

## Supplementary Figure S1

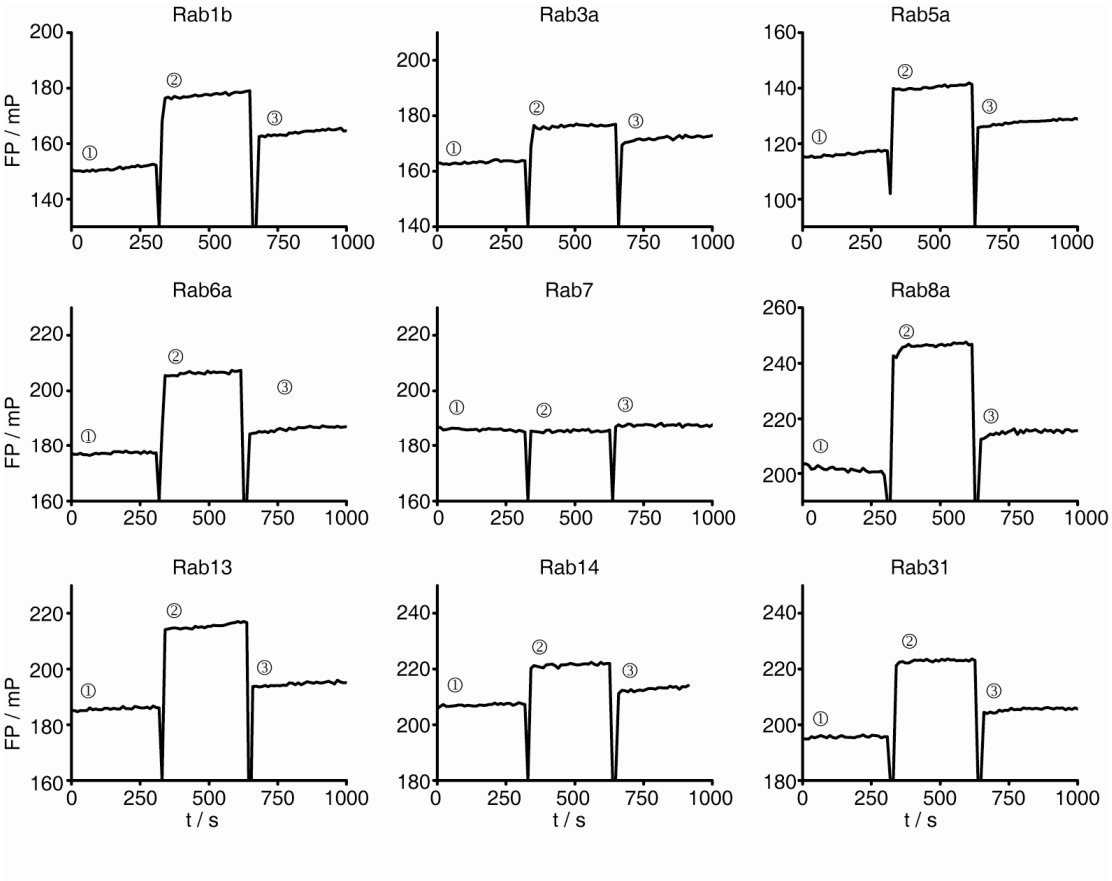


**Figure S1.** Interaction of OCRL1$_{539\text{-}901}$ with different Rab proteins. The Rab-binding activity of OCRL1 was examined by fluorescence polarization with different Rab proteins loaded with a fluorescent and non-hydrolyzable GTP analogue (mantGppNHp). Interaction between OCRL1$_{539\text{-}901}$ and RabX:mantGppNHp is indicated by an increase in fluorescence polarization. After 600 s, an excess of unlabeled Rab8:GppNHp was added to displace RabX:mantGppNHp from its complex with OCRL1$_{539\text{-}901}$. With the exception of Rab7, all Rab proteins tested (Rab1b, Rab3a, Rab5a, Rab6a, Rab8a, Rab13, Rab14 and Rab31) bind to OCRL1$_{539\text{-}901}$ (labeling: Addition of 5 µM fluorescent RabX:mantGppNHp (1), 5 µM OCRL1$_{539\text{-}901}$ (2) or 50 µM Rab8:GppNHp (3), respectively).

**Supplementary Figure S2**

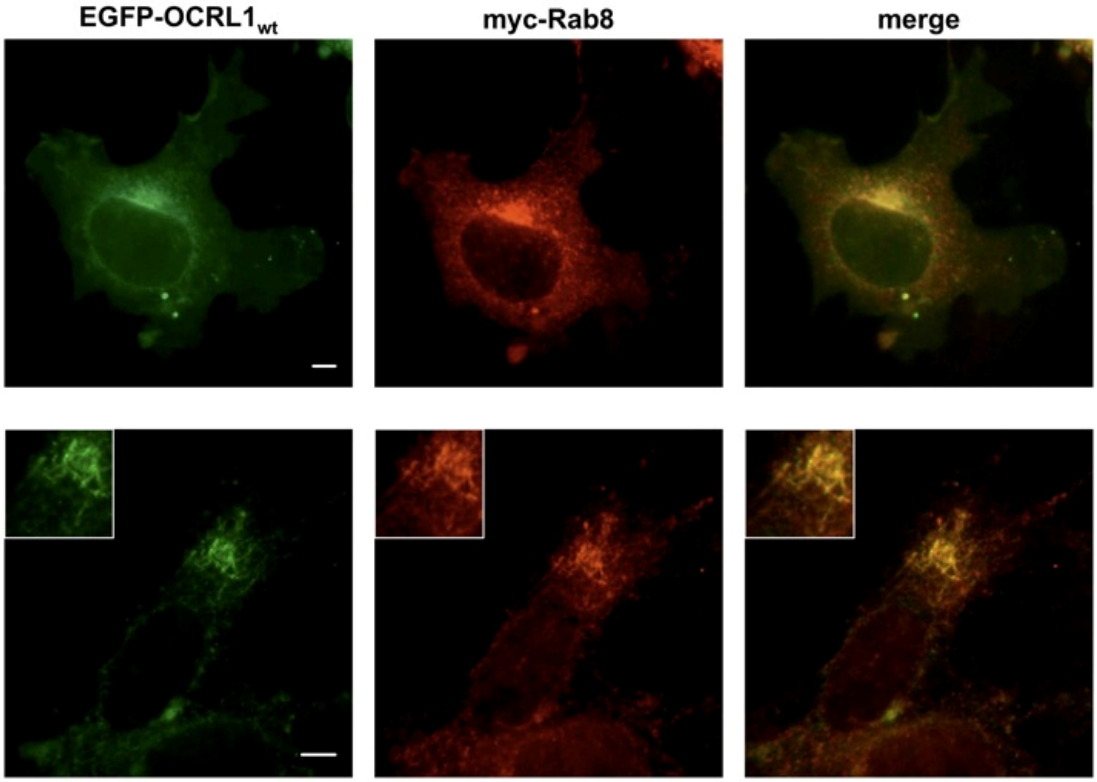


**Figure S2.** Colocalization of OCRL1 with Rab8a in Hela cells. Upper panel: Hela cells were co-transfected with expression constructs for EGFP-tagged OCRL1 and Myc-tagged Rab8a. 48 hours after transfection cells were fixed and analyzed with an anti-Myc antibody using immunofluorescence microscopy. The lower panel shows colocalization of EGFP-OCRL1 and Myc-Rab8a on membrane tubules, which are occasionally induced by overexpression of Rab8a. Insets show an enlargement of tubule network. (Bar, 10 μm).

**Supplementary Figure S3**

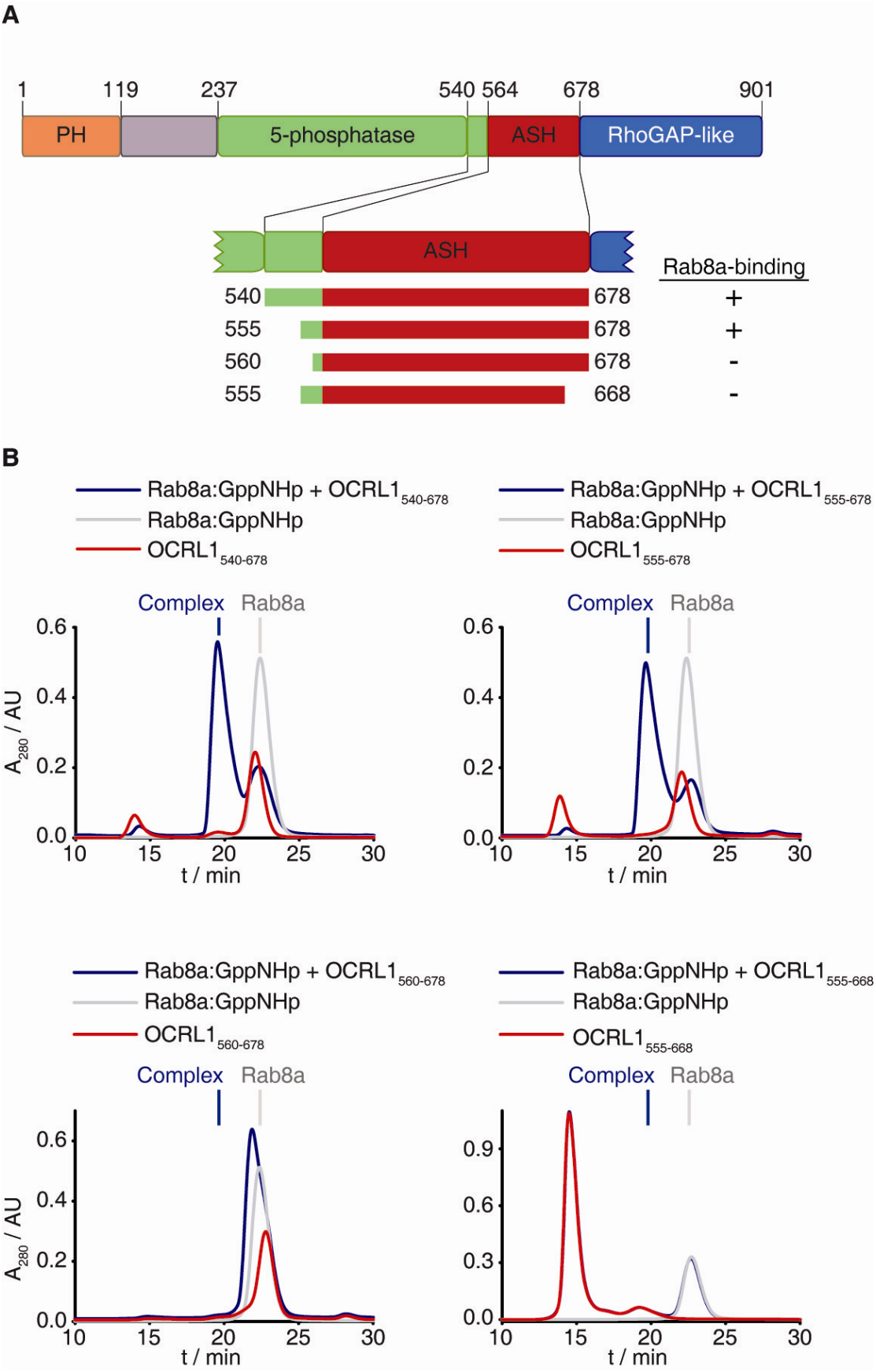

**Figure S3.** Complex formation of Rab8a:GppNHp with differently truncated OCRL1 constructs analyzed by size exclusion chromatography. (**A**) OCRL1 truncation constructs used to narrow down the Rab8a binding site The magnified depiction below the overall schematic structure indicates the various OCRL1 truncations used in the Rab8a binding experiments. (**B**) Gel filtration data of OCRL1 truncations complexes with Rab8a. 150 µg OCRL1 fragments ($OCRL1_{540-678}$, $OCRL1_{555-678}$, $OCRL1_{560-678}$ or $OCRL1_{555-668}$) were mixed with 300 µg Rab8a:GppNHp in a final volume of 110 µl. Complex formation was examined using an analytical gel filtration column (Superdex 75 10/30, GE Healthcare) monitored by UV absorption at 280 nm. Complex formation was observed for the constructs $OCRL1_{540-678}$ and $OCRL1_{555-678}$, but not $OCRL1_{560-678}$. $OCRL1_{555-668}$ aggregated due to instability.

**Supplementary Figure S4**

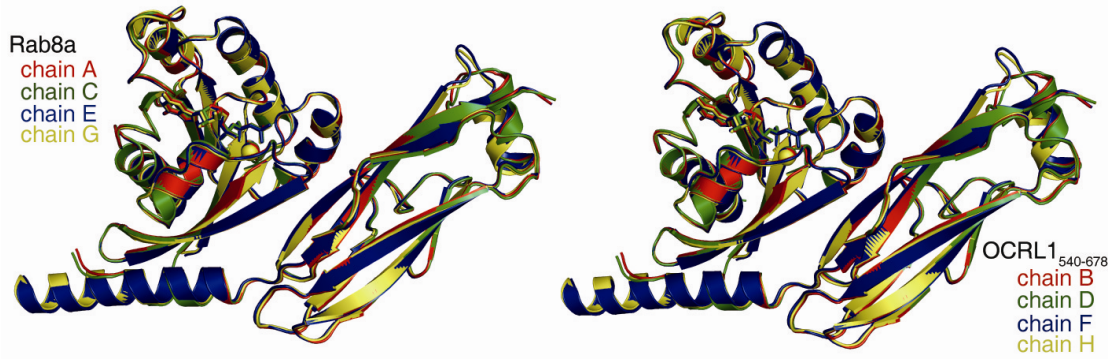


**Figure S4.** Stereo view of a structural superimposition of the four Rab8a:GppNHp:OCRL1$_{540-678}$ complexes in the asymmetric unit. Only OCRL1 residues 540-548 of chains B and D show significant differences compared to chains F and G. No electron density was seen for residues 540-548. The first amino acid of OCRL1 interacting with Rab8a is D555. Different chains are colored as indicated.

**Supplementary Figure S5**

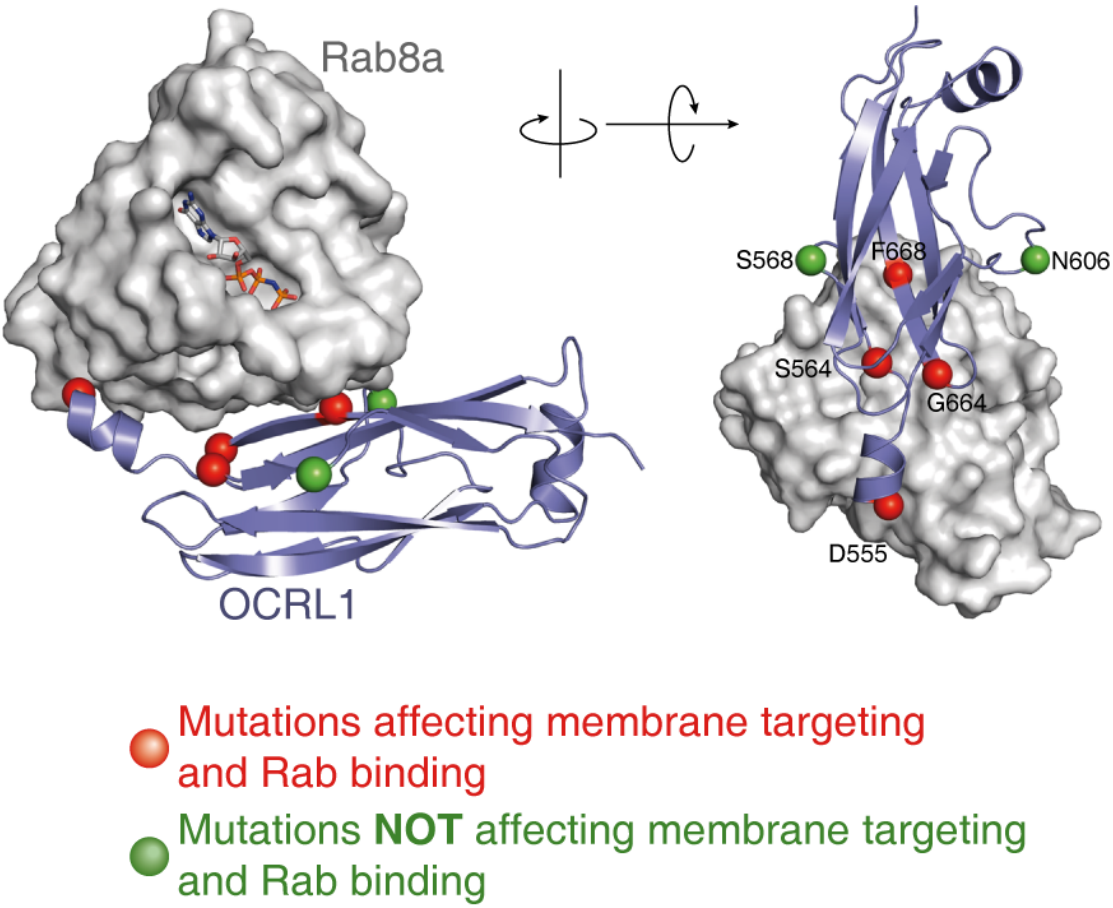


**Figure S5.** Previously analyzed OCRL1 mutants substantiate the validity of the observed Rab8a:OCRL1 complex interface. The Rab8a:OCRL1 complex structure is depicted (Rab8a: grey surface; OCLR1: blue cartoon). The amino acid positions of previously characterized OCRL1 substitutions (D555E, S568G, S564P, G664D, N606K, (Hyvola et al, 2006)) are indicated in sphere representation. Substitutions affecting Rab binding and OCLR1 membrane targeting are in red, whereas mutants showing Rab binding and membrane targeting indistinguishable from the wild type protein are in green. Additionally, the position of the Lowe syndrome mutation F668V is given (Swan et al, 2010). The mutations affecting Rab binding excellently align with the complex interface. (sticks: non-hydrolyzable GTP analogue (GppNHp; only amino acids 555-678 of OCRL1 are shown, corresponding to the minimal Rab-binding construct described in Figure S3)).

**Supplementary Figure S6**

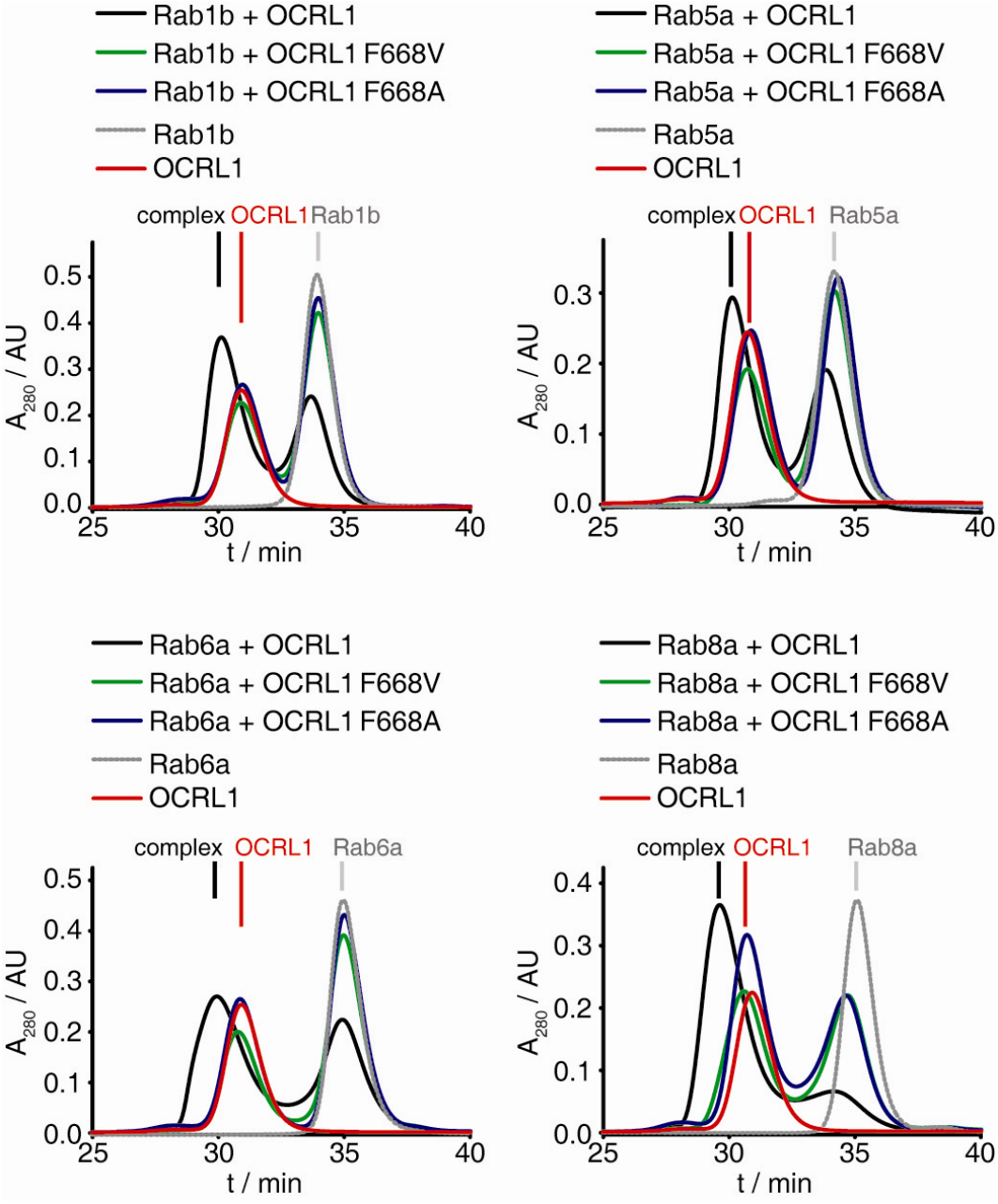


**Figure S6.** Complex formation of various GppNHp loaded Rabs with $OCRL1_{wt}$ and the F668V/F668A point mutants analyzed by size exclusion chromatography. The complexes were formed by incubating 150 µg active (GppNHp loaded) Rab protein (Rab1b, Rab5a, Rab6a and Rab8a) with 300 µg $OCRL1_{539\text{-}901}$, $OCRL1_{539\text{-}901}$F668V or $OCRL1_{539\text{-}901}$F668A, and separated on a Superdex200 10/30 column (GE Healthcare). The complex formation of the $OCRL1_{539\text{-}901}$ point mutants is abolished with Rab1b:GppNHp, Rab5a:GppNHp, and Rab6a:GppNHp and is greatly impaired with Rab8a:GppNHp.

**Supplementary references**

Hyvola N, Diao A, McKenzie E, Skippen A, Cockcroft S, Lowe M (2006) Membrane targeting and activation of the Lowe syndrome protein OCRL1 by rab GTPases. *EMBO J* **25**(16)**:** 3750-3761

Swan LE, Tomasini L, Pirruccello M, Lunardi J, De Camilli P (2010) Two closely related endocytic proteins that share a common OCRL-binding motif with APPL1. *Proc Natl Acad Sci U S A* **107**(8)**:** 3511-3516